



## ***Corrigendum to*** **“Environmental changes, climate and anthropogenic impact in south-east Tunisia during the last 8 kyr” published in *Clim. Past*, 12, 1339–1359, 2016**

**Sahbi Jaouadi<sup>1</sup>, Vincent Lebreton<sup>1</sup>, Viviane Bout-Roumazeilles<sup>2</sup>, Giuseppe Siani<sup>3</sup>, Rached Lakhdar<sup>4</sup>,  
Ridha Boussoffara<sup>5</sup>, Laurent Dezileau<sup>6</sup>, Nejib Kallel<sup>7</sup>, Beya Mannai-Tayech<sup>8</sup>, and Nathalie Combourieu-Nebout<sup>1</sup>**

<sup>1</sup>UMR 7194 CNRS, Histoire naturelle de l’Homme Préhistorique, Département de Préhistoire, Muséum national d’Histoire naturelle, Paris, France

<sup>2</sup>Laboratoire d’Océanologie et de Géosciences LOG, UMR8187, CNRS-Université Lille-Université Côte d’Opale, 59655 Villeneuve d’Ascq, France

<sup>3</sup>Laboratoire des Interactions et Dynamique des Environnements de Surface (IDES), UMR8148, CNRS-Université de Paris-Sud, Bat 504, 91405 Orsay CEDEX, France

<sup>4</sup>Faculté des Sciences de Bizerte, Université de Carthage, 7021 Zarzouna, Bizerte, Tunisia

<sup>5</sup>Institut National du Patrimoine, 4 Place du Château, 1008 Tunis, Tunisia

<sup>6</sup>UMR 5243 CNRS, Géosciences Montpellier, Université de Montpellier, Montpellier, France

<sup>7</sup>Université de Sfax, Faculté des Sciences, Laboratoire GEOGLOB, BP 802, 3038 Sfax, Tunisia

<sup>8</sup>Université de Tunis El Manar, Faculté des Sciences de Tunis, 2092 Tunis, Tunisia

*Correspondence to:* Sahbi Jaouadi (jaouadisahbi@yahoo.com)

Published: 23 June 2016

Figure 4 from this paper was originally published horizontally. However, for greater readability, the figure is presented vertically here.

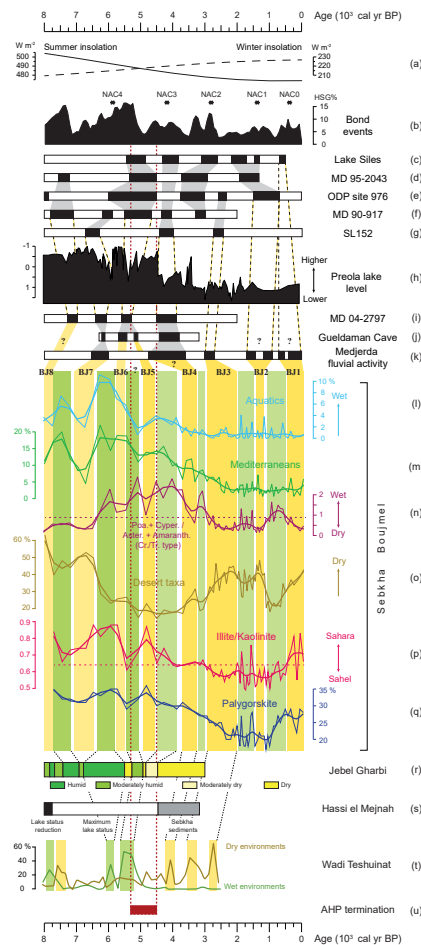


**Figure 4.** Comparison of pollen and clay mineralogy data from BJM2 core with paleoclimate records from the Mediterranean and the Sahara. **(a)** Summer (June mid-month) and winter (December mid-month) insolation ( $W m^{-2}$ ) curve at  $30^{\circ} N$  (Berger and Loutre, 1991). **(b)** Drift ice record from the North Atlantic: stacked percentage of HSG (hematite stained grains) of four records with stars indicate the North Atlantic cooling events (Bond et al., 2001; Bond et al., 1997). **(c)** Desiccation events at Lake Siles (southern Spain,  $38^{\circ}24' N$ ,  $2^{\circ}30' W$ ) based on *Pseudoschizaea* microfossil abundance (Carrión, 2002a). **(d)** Episodes of Mediterranean forest decline based on pollen data from MD 95-2043 core in the Alboran Sea ( $36^{\circ}9' N$ ,  $2^{\circ}37' W$ ) (Fletcher et al., 2012). **(e)** Temperate forest decline events ODP site 976 core in the Alboran Sea ( $36^{\circ}12' N$ ,  $4^{\circ}18' W$ ) (Combourieu Nebout et al., 2009). **(f)** Cold and dry events on core MD 90-917 ( $41^{\circ} N$ ,  $17^{\circ}37' E$ ) pollen record from the Adriatic Sea (Combourieu-Nebout et al., 2013). **(g)** Arid events from SL152 core (Aegean sea,  $40^{\circ}19' N$ ,  $24^{\circ}65' E$ ) (Kotthoff et al., 2008a, b; Schmiiedl et al., 2010). **(h)** Lake-level fluctuations (CA scores) at Lago Preola in Sicily ( $37^{\circ}37' N$ ,  $12^{\circ}38' E$ ) (Magny et al., 2011). **(i)** Identified arid spells on pollen data from MD 04-2797 core in the Siculo-Tunisian Strait ( $36^{\circ}57' N$ ,  $11^{\circ}40' E$ ) (Desprat et al., 2013). **(j)** Drought episodes based on stable isotopes record from stalagmite GLD1-stm4, Gueldaman Cave, N Algeria, ( $36^{\circ}26' N$ ,  $4^{\circ}34' E$ ) (Ruan et al., 2016). **(k)** Phases of increased fluvial activity with low soil formation and arid climate in the Medjerda River valley, northern Tunisia (Faust et al., 2004; Zielhofer et al., 2004). Pollen and clay mineralogy data from Sebkha Boujmel (BJM2 core,  $33^{\circ}16' N^{\circ}$ ,  $11^{\circ}05' E$ ) with bold lines showing the cubic smoothing splines and dashed lines averages for the I / K and W / D ratios. **(l)** Percentages of fresh water (Cyperaceae, *Glyceria*, *Juncus*, *Lemna*, *Potamogeton*, *Rumex aquaticus*-t., *Typhal/Sparganium*-t.) and **(m)** Mediterranean tree and shrub (*Buxus*, *Ceratonia*, *Cistus*, *Juniperus*, Lamiaceae, *Myrtus*, *Nerium*, *Olea*, Papaveraceae, *Pinus*, *Pistacia*, *Quercus ilex*-t., *Quercus deciduous*-t., *Rhus tripartita*-t.) pollen taxa. **(n)** Wet / dry (W / D) pollen ratio (Poaceae + Cyperaceae/Asteraceae Cichorioideae + Asteraceae Asteroideae + Amaranthaceae *Cornulacal/Traganum*-t.). **(o)** Percentages of desert pollen taxa (Apiaceae, *Asphodelus*, Asteraceae Asteroideae, Asteraceae Cichorioideae, *Calligonum*, *Capparis*, *Cistanche*, *Cleome*, *Cornulacal/Traganum*-t., Crassulaceae, Cucurbitaceae, *Echium*, *Ephedra distachia*-t., *Ephedra fragilis*-t., *Fagonia*, *Helianthemum*, Malvaceae, *Moltkiopsis ciliata*, *Neurada*, *Nitraria*, *Onosma*, *Reaumuria*, *Tamarix* and *Zygophyllum*). **(p)** Illite / kaolinite ratio and **(q)** palygorskite percentages. **(r)** Holocene climatic events in the Libyan Jeffara (Jebel Gharbi, north-western Libya,  $32^{\circ} N$ ) based on sedimentological and palynological data (Giraudi et al., 2013). **(s)** Paleohydrological changes at Hassi el Mejnah in Algeria ( $31^{\circ}14' N$ ,  $2^{\circ}30' E$ ) (Gasse, 2002; Hoelzmann et al., 2004). **(t)** Pollen data from rock shelters in the Wadi Teshuinat area (Tadrart Acacus Massif, central Sahara, south-west Libya ( $24^{\circ}30' - 26^{\circ} N$ ,  $10 - 12^{\circ} E$ ; Cremaschi et al., 2014; Mercuri, 2008). **(u)** Estimated duration of the African Humid Period termination ( $4.9 ka \pm 400, 2\sigma$ ) as indicated by aeolian dust flux data on marine sediment cores from the north-west African margin (McGee et al., 2013).